

RNA

RNase III autoregulation: structure and function of rncO, the posttranscriptional "operator"

J. Matsunaga, E. L. Simons and R. W. Simons

RNA 1996 2: 1228-1240

References

Article cited in:

<http://www.rnajournal.org/cgi/content/abstract/2/12/1228#otherarticles>

Email alerting service

Receive free email alerts when new articles cite this article - sign up in the box at the top right corner of the article or [click here](#)

Notes

To subscribe to *RNA* go to:
<http://www.rnajournal.org/subscriptions/>

RNase III autoregulation: Structure and function of *rncO*, the posttranscriptional “operator”

JAMES MATSUNAGA, ELIZABETH L. SIMONS, and ROBERT W. SIMONS

Department of Microbiology and Molecular Genetics and the Molecular Biology Institute,
University of California, Los Angeles, California 90095, USA

ABSTRACT

Expression of the *Escherichia coli rnc-era-recO* operon is regulated posttranscriptionally by ribonuclease III (RNase III), encoded in the *rnc* gene. RNase III initiates rapid decay of the *rnc* operon mRNA by cleaving a double-stranded region of the *rnc* leader. This region, termed *rncO*, is portable, conferring stability and RNase III regulation to heterologous RNAs. Here, we report the detailed analysis of *rncO* structure and function. The first 215 nt of the *rnc* leader are sufficient for its function. Dimethylsulfate (DMS) modification *in vivo* revealed distinct structural elements in this region: a 13-nt single-stranded 5' leader, followed by a 6-bp stem-loop structure (I), a larger stem-loop structure (II) containing the RNase III site, a single-stranded region containing the *rnc* translation initiation site, and a small stem-loop structure (III) at the 3' terminus of *rncO*, wholly within the *rnc* coding region. Genetic analysis revealed the function of these structural elements. The single-stranded leader is not required for stability or RNase III control, stem-loop II is required only for RNase III control, and both stem-loops I and III are required for stability. Stem-loop II effectively serves only as the site at which RNase III cleaves to remove stem-loop I and thereby initiates decay, after which RNase III plays no role. Mutations at the cleavage site underscore the importance of base pairing for efficient RNase III attack. When stem-loops I and II were replaced with an artificial hairpin structure, stability was restored only partially, but was restored almost fully when a single-stranded leader was also added.

Keywords: gene expression; posttranscriptional control; ribonuclease III; RNA degradation; RNA structure

INTRODUCTION

The decay of most messenger RNAs in *Escherichia coli* is thought to initiate with endonuclease cleavage at one or a few specific sites, often near the 5' end, followed by rounds of 3'-exonuclease and additional endonuclease attack on the intermediate decay products (Ehretsmann et al., 1992; Belasco, 1993). Secondary structures at the 5' end can also impart stability (Gorski et al., 1985; Emory et al., 1992). Deletion of stem-loop structures in the *ompA* mRNA leader reduced transcript stability significantly, whereas their replacement with an artificial hairpin structure restored stability (Emory et al., 1992). Addition of five or more unpaired nucleotides to the 5' end of the native *ompA* transcript also reduced stability (Emory et al., 1992). These observations led to the proposal that mRNA decay generally initiates when the 5'-terminal single-stranded region of a tran-

script is bound by a ribonuclease that subsequently makes internal cuts, and that such attack is blocked if the 5' terminus is base paired (Emory et al., 1992). Importantly, the 5' leader and first 20 codons of the *ompA* message confer stability to the heterologous *bla*, *phoA*, *cat*, and *lacZ* mRNAs, showing that the *ompA* leader is a portable stability element that protects mRNAs from a common decay pathway (Hansen et al., 1994).

Expression of the *E. coli rnc* operon is autoregulated negatively at the level of transcript stability (Bardwell et al. 1989; Matsunaga et al., 1996). The first gene of the operon (*rnc*; see Fig. 1) encodes ribonuclease III (RNase III), a double-stranded RNA (dsRNA)-specific endonuclease involved in ribosomal and messenger RNA processing and decay (Court, 1993; Nicholson, 1996). The second gene, *era*, encodes a small, essential GTP-binding protein of unknown function (Ahnn et al., 1986; March et al., 1988), and the third, *recO*, is involved in plasmid recombination (Kolodner et al., 1985). RNase III cleaves both strands of a single, dsRNA region in the *rnc* mRNA leader (sites R1 and R2; Fig. 1), initiating rapid decay of downstream sequences and re-

Reprint requests to: Robert W. Simons, Department of Microbiology and Molecular Genetics, 1602 Molecular Science, University of California, Los Angeles, California 90095, USA; e-mail: bobs@microbio.lifesci.ucla.edu.

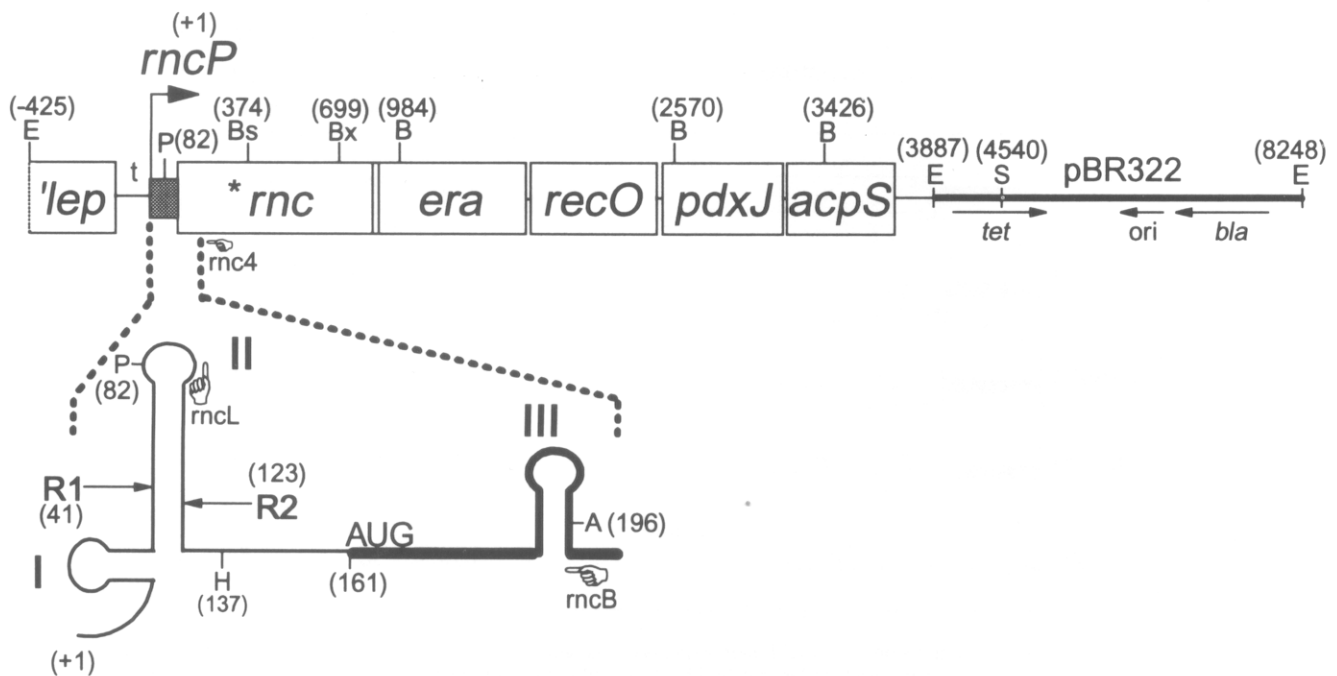


FIGURE 1. The *rnc* operon and downstream genes. Shown is a 4,312-bp *Eco*R I fragment from the *E. coli* chromosome inserted into the *Eco*R I site of pBR322, producing plasmid pACS1 (Takiiff et al., 1989). This fragment contains the intact *rnc*, *era*, *recO*, *pdxJ*, and *acpS* genes and a portion of the upstream leader peptidase gene (*'lep*), oriented left-to-right (not to scale) and numbered from the start-point of *rnc* operon transcription (Matsunaga et al., 1996). The *bla* (ampicillin resistance), *tet* (tetracycline resistance), and *ori* (replication origin) genes of pBR322 are also shown. The entire sequence of the plasmid is known. The bent arrow indicates the initiation site for the *rncP* promoter. The 5' untranslated region of the *rnc* operon is hatched. *rncO* comprises the first 378 nt (or less) of the *rnc* operon and contains stem-loop structures I, II, and III, depicted schematically (see Fig. 5 for details). RNase III cleaves at sites R1 (between nt 40 and 41) and R2 (nt 122 and 123) in stem-loop II (Bardwell et al., 1989). The initial portion of the *rnc* coding region is shown as a heavy line. The cartoon hands indicate the orientation and approximate position of several oligonucleotide primers, whose 5'-3' coordinates are *rncL* (101-79), *rnc4* (266-249), and *rncB* (211-199). Selected restriction sites are: A, *Alu* I; B, *Bam*H I; Bs, *Bss*H II; Bx, *Bst*X I; E, *Eco*R I; H, *Hinc* II; P, *Pst* I; S, *Sal* I. An asterisk marks the *rnc105* point mutation (+290) present in the isogenic plasmid pACS1*rnc105*.

ducing both *rnc* and *era* expression (Bardwell et al., 1989; Matsunaga et al., 1996). When fused to the heterologous *lacZ* mRNA, the first 378 nt of *rnc* mRNA confer increased stability in the absence of RNase III, and contain all of the *cis*-acting elements necessary for regulation by RNase III (Matsunaga et al., 1996). We term this portable, regulated, 5' stability element *rncO*, in light of its functional similarity to transcriptional and translational operators. Here, we determine *rncO* RNA secondary structure *in vivo*, define more precisely the minimum sequence required for its function, dissect the function of its substructural elements, and define precisely the role of RNase III.

RESULTS

The minimal *rncO* sequence

We showed previously that the first 378 nt of the *rnc* mRNA are sufficient to stabilize the *lacZ* message and render it sensitive to RNase III regulation (Matsunaga

et al., 1996). To further define the limits of *rncO*, the *rnc* gene was deleted at various positions just downstream of the start of transcription (+1) (see Fig. 1) and fused in-frame to the truncated '*lacZ*' reporter gene, creating a set of related protein (translational) fusions and, in effect, an isogenic set of 3' *rnc* deletions (see Fig. 2). These fusions were then placed in single copy in the chromosomes of *rnc*⁺ (P90C) and *rnc14* (RS6521) cells and their levels of expression measured (Fig. 2; *rnc14* abolishes RNase III activity). Fusions containing the first 205, 215, 226, or 378 nt of the *rnc* mRNA were all regulated 7–8-fold by RNase III, whereas the fusion containing only the first 196 nt was not (\approx 1.5-fold). We also noticed that, in the absence of RNase III, expression from the +196 fusion was 4–5-fold lower than that of fusions +215 or longer.

Primer extension analysis showed parallel effects on *rnc*'-'*lacZ* mRNA levels (Fig. 3A). Hybrid mRNAs containing 205 nt or more of *rnc* sequence were cleaved efficiently by RNase III (Fig. 3A; cf. lanes 3–6 with lanes 9–12; results with the +205 and +378 fusions were similar). In each case, the band corresponding to the de

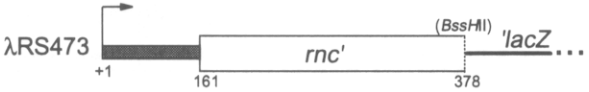
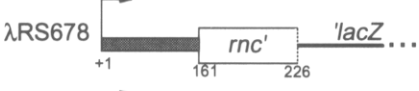
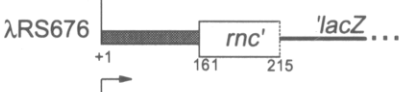
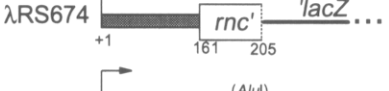
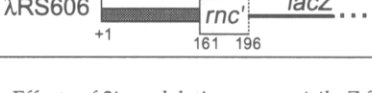
fusion structure	protein fusion expression		
	units β -gal <i>rnc14</i>	<i>rnc</i> ⁺	fold control
 λ RS473	560	65	8.6x
 λ RS678	735	115	6.4x
 λ RS676	635	80	7.9x
 λ RS674	285	40	7.1x
 λ RS606	150	95	1.6x

FIGURE 2. Effects of 3' *rnc* deletions on *rnc*'-*lacZ* fusion expression. Isogenic *rnc*'-*lacZ* protein fusions containing the intact *rnc* promoter (+1; arrow) and untranslated leader (hatched box), but different portions of the *rnc* coding region (open boxes), were constructed and analyzed in single copy on the chromosomes of RS6521 (*rnc14*) and P90C (*rnc*⁺). Fusion junctions are numbered from +1. Thick lines indicate '*lacZ*'. The *rnc* start codon is at +161. β -Galactosidase activities were determined as described (Matsunaga et al., 1996), and the values shown are the averages of at least three independent determinations (standard deviations were <10% of the means). λ RS473 has been described (Matsunaga et al., 1996). λ RS606 was constructed in the same way, using the *Alu* I site at +196. The remaining fusions were constructed by first generating PCR products with pRS1398 (*rnc*⁺) template and appropriate primers. These products were then inserted into pRS414 to create the *rnc*'-*lacZ* protein fusions shown, crossed to λ RS45 by homologous recombination, and the resulting phages integrated at the λ *att* sites of P90C and RS6521, all as described (Simons et al., 1987).

novo 5' terminus (+1) was replaced by lower levels of the band corresponding to the downstream RNase III cleavage site, R2 (see Fig. 1), a pattern that is characteristic of normal RNase III autoregulation of both intact and fusion mRNAs, and reflects the lower stability of the cleaved species (Bardwell et al., 1989; Matsunaga et al., 1996). In contrast, whereas fusion transcripts containing only the first 166 or 196 nt of *rnc* were cleaved efficiently, the relative intensities of their +1 and R2 bands remained about the same (Fig. 3A; cf. lanes 1 and 2 with 7 and 8, and lane 13 with 14). Thus, RNase III cleavage and transcript destabilization are genetically separable (see below).

When these same *rnc* sequences were fused in-frame to a truncated '*kan*' gene and analyzed by primer extension, the +215 and +226 hybrid transcripts were regulated normally (Fig. 3B, lanes 1–4), but the +166 mRNA was not (lanes 9 and 10), consistent with effects on the corresponding *lacZ* fusions. However, both the +196 and +205 mRNAs were regulated at intermediate levels (lanes 5–9), unlike the corresponding *lacZ* fusions (where +205 is regulated but +196 is not). Therefore, +215 is the shortest *rnc* sequence that is regulated normally when fused to either '*lacZ*' or '*kan*'.

To determine if regulation of these fusions is occurring at the level of message stability per se, we measured the metabolic half-lives of several *rnc*'-*lacZ*

fusion transcripts in *rnc*⁺ and *rnc14* cells after the addition of rifampicin to inhibit new transcription. The half-life of +215 and +226 mRNAs was \approx 3.5 min in the absence of RNase III, but only \approx 0.5 min in its presence (Table 1), as seen previously for intact *rnc* mRNA and the *rnc*'-*lacZ* hybrid mRNA fused at +378 (Matsunaga et al., 1996), and close to the stability of native *lacZ* mRNA (Kennell & Reizman, 1977; Cannistraro et al.,

TABLE 1. Half-lives of *rnc*'-*lacZ* fusion mRNAs.

<i>rnc</i> '- <i>lacZ</i> prophage ^a	Fusion junction ^a	Half-life (min) in <i>E. coli</i> host ^b		Fold control ^c
		<i>rnc14</i>	<i>rnc</i> ⁺	
λ RS678	+226	3.3	0.65	5.1x
λ RS676	+215	4.0	0.66	6.1x
λ RS606	+196	1.1	0.98	1.1x

^a See Figure 2.

^b Half-lives were determined (after the addition of rifampicin to inhibit new transcription) by primer extension analysis (with the *lacZ1* oligonucleotide) of total cellular RNA extracted from P90C (*rnc*⁺) or RS6521 (*rnc14*) cells containing the indicated single-copy prophages, as described (Matsunaga et al., 1996). The +1 band was quantitated in the *rnc14* case; R2 was quantitated in the *rnc*⁺ case (see Fig. 3).

^c Fold control is the ratio of *rnc* transcripts half-lives in *rnc14* and *rnc*⁺ cells in each case.

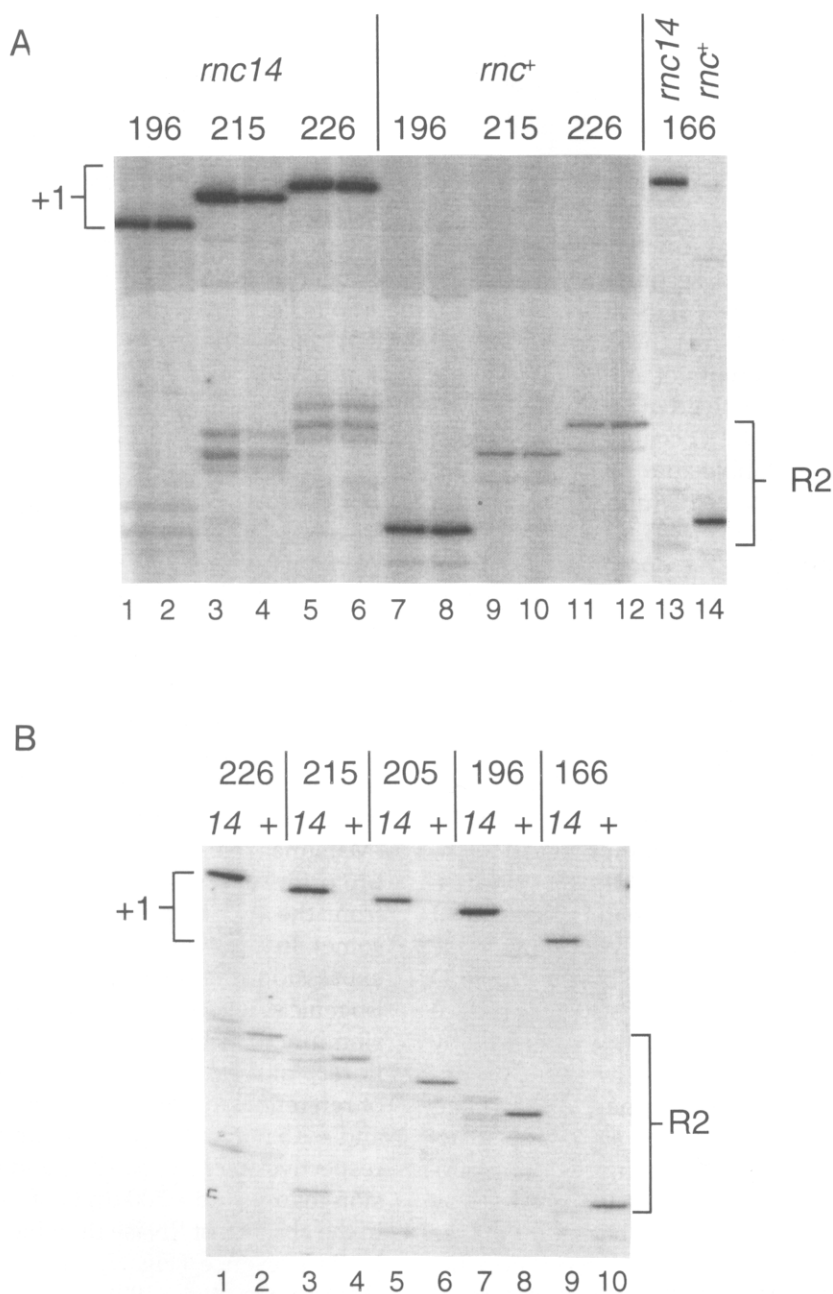


FIGURE 3. Effects of 3' deletions on fusion mRNA levels and decay. **A:** *rnc⁺*-*lacZ* fusions. Total RNA was extracted from RS6521 (*rnc14*) and P90C (*rnc⁺*) cells lysogenized or transformed with *rnc⁺*-*lacZ* fusions containing the first 166, 196, 215, or 226 nt of the *rnc* gene, and analyzed by primer extension (two independent samples) with an oligonucleotide (*lacZ*1) complementary to an early portion of the *lacZ* mRNA, as described (Matsunaga et al., 1996). Bands corresponding to the transcription start site (+1) and the downstream RNase III cleavage site (R2; Bardwell et al., 1989) are indicated. The +166 *rnc⁺*-*lacZ* fusion was carried on pRS2730 and was constructed as described in Figure 2. The remaining fusions were borne on the recombinant prophages described in Figure 2. For these latter cases, similar results were obtained with the corresponding plasmid-borne fusions (not shown). **B:** *rnc⁺*-*kan* fusions. Total RNA extracted from cells transformed with corresponding *rnc⁺*-*kan* fusions was analyzed similarly, using a primer (*kan*1) complementary to an early portion of the *kan* mRNA. Plasmids were constructed as described in Figure 2, except that *rnc* fragments were inserted into pRS1272 (Sussman et al., 1990) to create *rnc⁺*-*kan* fusions with the following fusion junctions: pRS2703 (+226); pRS2702 (+215); pRS2701 (+205); pRS2700 (+196); pRS3057 (+166).

1986; Peterson, 1991). On the other hand, in the absence of RNase III, the +196 hybrid transcript was already ≈ 4 -fold less stable than the +215 mRNA, and not further destabilized in the presence of RNase III

(Table 1). Moreover, the stability of the +196 hybrid mRNA is, itself, close to that of the native *lacZ* message. Taken together, these results show that deletion of *rnc* sequence between +215 and +196 removes or

disrupts some element required for the stability of *rnc'*-*lacZ* transcripts in the absence of RNase III, and that, in the absence of such stabilization (or the element itself), RNase III cleavage is no longer destabilizing.

***rncO* secondary structure**

Prior to examining individual functional elements in *rncO*, we determined its RNA secondary structure by examining dimethylsulfate (DMS) methylation in vivo. DMS methylates adenines (A) at the N1 position and cytosines (C) at N3 (Ehresmann et al., 1987). Because both of these groups are involved in normal base pairing, methylation of As and Cs occurs more readily in single-stranded than in double-stranded regions, providing a means to probe RNA structure. RS6521 (*rnc14*) was transformed with pACS1*rnc105*, a multicopy plasmid that contains the entire *rnc* operon and harbors the *rnc105* point mutation (Fig. 1), which inactivates RNase III activity, maps well downstream of *rncO*, and does not alter RNase III regulation in *cis* (Bardwell et al., 1989; Matsunaga et al., 1996). Total cellular RNA was extracted from transformants incubated with DMS and then analyzed by primer extension to reveal the predominant sites of RNA methylation (Inoue & Cech, 1985). Typical results are shown in Figure 4. For the first 215 nt of *rnc* mRNA, which comprise the 5' untranslated leader and the first 55 nt of the *rnc* gene, we found that the DMS modification pattern was most consistent with the thermodynamically most favorable RNA secondary structure predicted by the MFOLD computer program (Zuker, 1989). This structure (Fig. 5) contains a 13-nt 5' single-stranded leader followed by two imperfect stem-loop structures (I and II), an unpaired region containing the *rnc* Shine-Dalgarno and initiation codon (AUG), and an 8-bp stem-loop structure (III) located within the *rnc* coding region. Structure II, which is identical to the structure proposed by Bardwell et al. (1989), is arbitrarily divided into three substructures, stems IIa and IIb and stem-loop IIc. Stem IIa contains the R1 and R2 sites of RNase III cleavage.

The salient DMS results can be summarized as follows. (1) All four A's in the predicted 5' single-stranded region were methylated (Fig. 4A). (2) None of the five C's predicted in the stem of structure I were modified, although an A opposite a bulge and another at the base were (Fig. 4A). (3) The A and two C's in loop I were modified. (4) None of the A's or C's in the 15 bp of stem IIa (the site of RNase III cleavage) was strongly modified (Fig. 4A,B), consistent with RNase III's requirement for a dsRNA substrate (Nicholson, 1996). (5) All of the A's and nearly all of the C's between stem-loops II and III were methylated (Fig. 4B,C), indicating that most of this region, which includes the ribosome-binding site, is single-stranded. (6) Three C's in stem III were unmodified (Fig. 4C), but the remaining

C and two A's were, suggesting that structure III is in equilibrium with its unfolded conformation (possibly due to elongating ribosomes). When RNA was first extracted from RS6521/pACS1*rnc105* and then treated with DMS in vitro, the modification pattern (not shown) was nearly identical to that obtained with RNA modified in vivo.

Further support for the structure shown in Figure 5 came from a phylogenetic comparison with the *Salmonella typhimurium rnc* gene sequence (P. Anderson & R.W. Simons, in prep.). The *Salmonella rncO* structure is predicted to contain a nearly identical stem-loop I (differing by only a GC to AU covariance in the stem) and identical stem IIa and stem-loops IIc and III.

Functional dissection of *rncO*

Working from the *rncO* secondary structure, we created and examined several *rncO* deletions in order to define which sequences or structures are involved in determining the stability and RNase III regulation of the *rnc* mRNA. Deletions were introduced into pACS1*rnc105*, transformed into RS6521 (*rnc14*) or P90C (*rnc*⁺) cells, total cellular RNA extracted and analyzed by primer extension, and half-lives of the *rnc* mRNA determined using oligonucleotide *rnc4* (see Fig. 1), as described (Matsunaga et al., 1996). The results are shown in Figure 6 (in all cases, the predominant signals derived from the multicopy plasmid, not the host chromosome). In addition, to measure their effects on *rnc* gene expression, the deletions were also incorporated into isogenic single-copy *rnc'*-*lacZ* protein fusions (with fusion junctions at +378) and their levels of expression in *rnc*⁺ and *rnc14* hosts measured (Fig. 7). For points of reference, the *rncO*⁺ transcript half-lives were ≈0.5 and ≈2.5 min in the presence and absence of RNase III, respectively (Fig. 6; *rncO*⁺), and the corresponding fusion manifested ≈500 units of β-galactosidase activity in the absence of RNase III, which was reduced ≈4-fold in its presence (Fig. 7; *rncO*⁺), as seen previously (Matsunaga et al., 1996).

The *rncO*Δ(1-*R2*) mutation replaces *rncP* and the sequence between the transcription start-site and the downstream RNase III cleavage site (*R2*) with the heterologous pOUT_{C8} promoter from IS10 (Case et al., 1988). This caused transcription to initiate at G residues 2 nt upstream and 1 nt downstream of *R2*. Presumably, both of these species bear 5' triphosphates. Thus, the *rncO*Δ(1-*R2*) RNAs closely resemble (but are not identical to) the normal RNase III-cleaved *rnc* transcript. In the absence of RNase III, *rncO*Δ(1-*R2*) reduced *rnc* transcript stability ≈3-fold (Fig. 6), consistent with disruption or removal of an element required for intrinsic *rnc* mRNA stability. Furthermore, RNase III control of RNA stability (Fig. 6) and fusion expression (Fig. 7) was reduced to ≈1.4-fold, consistent with removal of the RNase III cleavage site. These results suggest

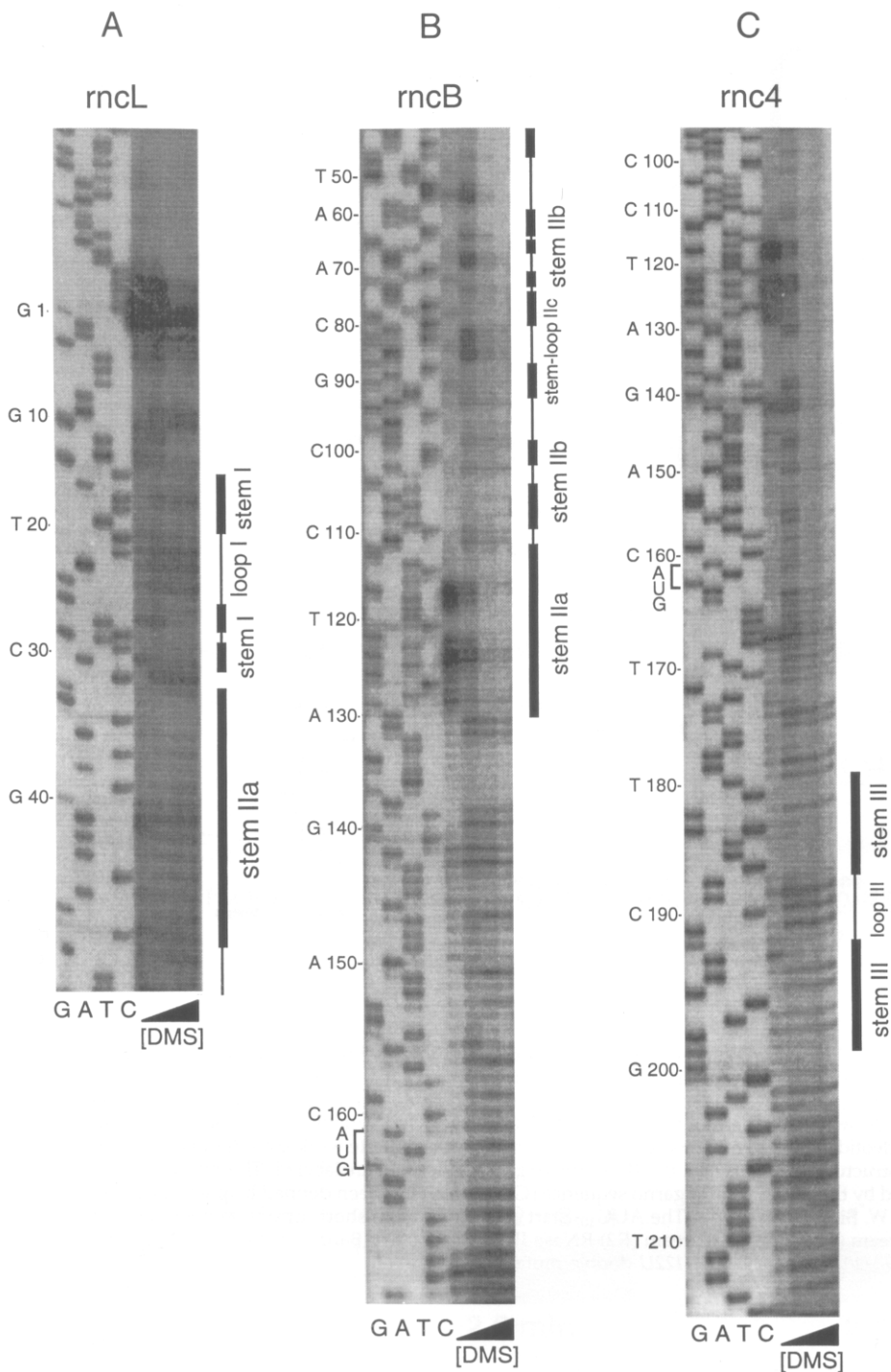


FIGURE 4. DMS modification of the *mc* leader in vivo. RS6521 (*rnc14*) cells transformed with pACS1*rnc105* were treated with DMS as described by Mayford and Weisblum (1989), except that the final DMS concentrations were (left to right) 0, 0.2, 1, and 2% by volume, and all incubations were for 5 min at 37°. Total cellular RNA was then extracted and analyzed by primer extension with oligonucleotides (A) *rncL*, (B) *rncB*, and (C) *rnc4*. Nucleotide sequence (numbered from the start point or *mc* transcription; +1) was generated with the same primers using pRS2249 (Matsunaga et al., 1996) as template. Regions corresponding to elements of structures I, II, and III (see Fig. 5) are indicated, where the thick and thin lines represent paired and unpaired nucleotides, respectively.

strongly that RNase III plays little or no role in *rnc* stability or expression once *rncO* is cleaved.

When structure II was deleted at its base [*rncO* Δ (II)], there was no reduction in *rnc* mRNA stability or fusion expression in the absence of RNase III, and no evidence of RNase III control (Figs. 6, 7; Δ II). Neither was there evidence of RNase III cleavage (Fig. 8A; cf. lanes 3 and 4 with 11 and 12). The presence of a putative primer-extension pause product corresponding to the 3' margin of structure I suggests that it remains

intact when structure II is deleted (Fig. 8A; bands marked with * in lanes 3, 4 and 11, 12).

Deletion of the first 10 nt of the leader in *rncO* Δ (ss) had very little effect on either transcript stability or fusion expression, or on regulation by RNase III (Figs. 6, 7; Δ ss). Therefore, the short, 5'-terminal single-stranded leader appears to play no role in determining *rnc* mRNA stability or control.

The different effects of the *rncO* Δ (1-R2) and *rncO* Δ (II) mutations reveal the essential functions of *rncO*. Struc-

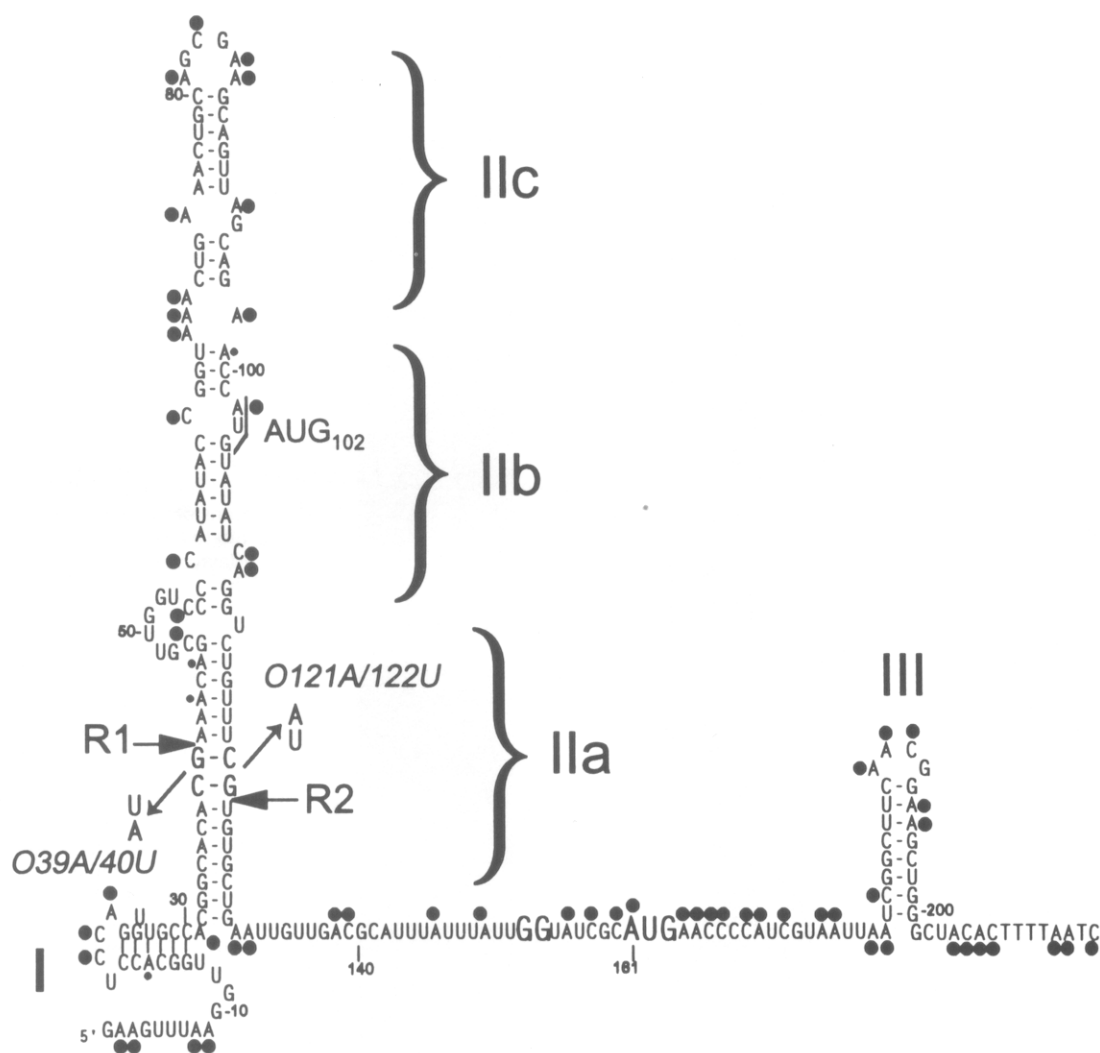


FIGURE 5. Secondary structure of *mco*. The RNA secondary structure of the leader and beginning of the *mrc* gene (the first 215 nt, numbered from the start point of *mrcP* transcription) was determined by comparing the pattern of DMS modification of *mrc* mRNA expressed in vivo (see Fig. 4 for typical results) with RNA secondary structures predicted by the MFOLD computer program (Zuker, 1989). Shown is the thermodynamically most stable predicted structure, which also fit the empirical data best. Dots indicate nucleotides consistently modified by DMS (smaller dots indicate weaker modification). Stem-loop structures I, III, and the substructural elements (IIa, IIb, IIc) of the larger stem-loop II, are labeled. The *mrc* start codon (AUG) is at position 161, preceded by the Shine and Dalgarno sequence (GG), which has been defined by point mutation (J. Matsunaga, E.L. Simons, & R.W. Simons, in prep.). The AUG₁₀₂ start codon initiates a short, upstream open reading frame. Arrows point to the upstream (R1) and downstream (R2) RNase III cleavage sites (Bardwell et al., 1989) and the nucleotide changes in the *mrcO39A/40U* and *mrcO121A/122U* double mutations.

ture II is not required for intrinsic stability. However, in its absence, structure I is required (although it may not be required in the presence of structure II). Therefore, from a practical perspective, structure I is the primary stabilizing element in *mco*, and structure II serves as the substrate for RNase III cleavage and the means by which structure I (along with structure II) is removed.

A heterologous stem-loop structure is a modest 5' stability element

Emory et al. (1992) showed that an artificial hairpin structure comprised of a 14-bp stem and a 4-nt loop

could functionally replace the native stem-loop structures at the 5' end of the *E. coli ompA* mRNA, so long as there was not also a single-stranded 5' leader. We used this same structure, with (SHP) and without (HP) a putative 10-nt single-stranded leader, to replace the first 122 nt of the *mrc* leader, in effect attaching HP or SHP at the R2 site of RNase III cleavage. These substitutions were then examined as described above (Figs. 6, 7; HP, SHP). In the absence of RNase III, both HP and SHP increased transcript stability and fusion expression to intermediate levels relative to *mrcOΔ* (1-R2), *mrcOΔ*(II), and *mrcO*⁺. As expected, neither substitution mutant was regulated greatly by RNase III

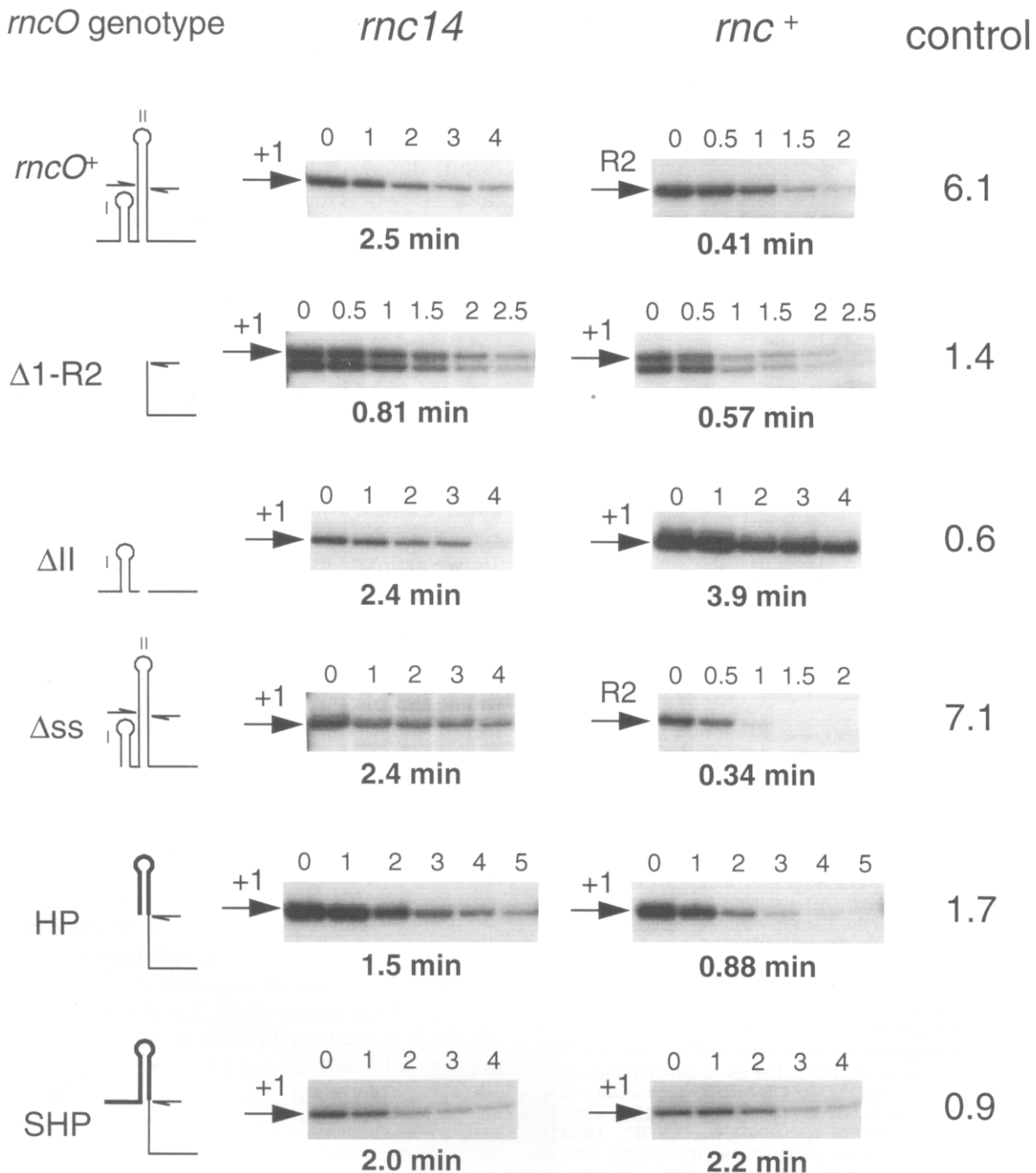


FIGURE 6. Effects of *rncO* mutations on mRNA decay rates. RNA extracted from RS6521 (*rnc14*) and P90C (*rnc*⁺) cells transformed with multicopy plasmids containing wild-type or mutant *rncO* elements was analyzed by primer extension with oligonucleotide *rnc4*, and the metabolic half-lives of the +1 or R2 bands (in the absence and presence of RNase III cleavage, respectively) were determined as described (Table 1; Case et al. 1990; Matsunaga et al., 1996). Drawings depict known or putative RNA secondary structure(s) in each case. Thin and thick lines represent *rnc* leader and synthetic sequences, respectively, and the gap indicates an internal deletion. Stem-loops I and II of *rncO* (see Fig. 5) are labeled when present (stem-loop III is always present but not shown). The half-arrows indicate the R1 and R2 cleavage sites, although cleavage does not occur in all cases (see text). Each panel shows the decay of the +1 or R2 bands following the addition of rifampicin (in minutes), with the calculated half-lives shown below. "Control" is the ratio of half-lives in *rnc*⁺ and *rnc14* cells. The sequence of the artificial hairpin (HP) is 5'-GAUCGCCCCACCGGC[AGCU]GCCGGUGGGCGAUC, with the predicted loop bracketed. The sequence of the additional single-stranded 5' leader in SHP is 5'-GAACAUAGGC. Plasmids (all isogenic to pACS1*rnc105*) were pRS2735 [*rncO*Δ(1-R2)], pRS3091 [*rncO*Δ(II)], pRS3085 [*rncO*Δ(ss)], pRS3123 [*rncO*(HP)], and pRS3124 [*rncO*(SHP)], and their construction is described in the Materials and methods.











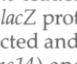
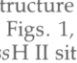
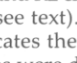
<i>rncO</i> genotype	<i>rncO</i> structure	β -galactosidase		fold control
		<i>rnc14</i>	<i>rnc</i> ⁺	
<i>rncO</i> ⁺		510	120	4.3x
Δ 1-R2		45	35	1.3x
Δ II		940	965	1.0x
Δ ss		675	80	8.4x
HP		185	270	0.7x
SHP		350	525	0.7x
<i>rncO39A/40U</i>		455	600	0.8x
<i>rncO221A/222U</i>		390	505	0.8x
<i>rncO39A/40U/221A/222U</i>		365	105	3.5x
<i>rncO</i> ⁺		530	80	6.6x
Δ 78-81		385	65	5.9x
Δ 78-81ins		410	80	5.1x
ACG ₁₀₂		415	70	5.9x

FIGURE 7. Effects of *rnc* leader mutations on *rnc*'-*lacZ* fusion expression. Isogenic *rnc*'-*lacZ* protein fusions containing different *rncO* mutations were constructed and analyzed in single copy on the chromosomes of RS6521 (*rnc14*) and P90C (*rnc*⁺). For each, the known or putative secondary structure of the leader is shown schematically as in Figure 6 (also see Figs. 1, 5). All fusions contain identical fusion junctions at the *Bss*H II site of *rnc* (+378, see Fig. 1). The half-arrows indicate the R1 and R2 cleavage sites, although cleavage does not occur in all cases (see text). Asterisks indicate point mutations and solid triangle indicates the 12-nt insertion in *rncO* Δ (78-81ins). β -galactosidase activities were determined as in Figure 2. "Fold control" is the ratio of fusion expression in *rnc*⁺ and *rnc14* cells in each case. All fusions were constructed by inserting appropriate fragments (after first replacing the *Bss*H II site with a *Bam*H I linker to assure in-frame fusion) into pRS414, crossed to λ RS45 by homologous recombination and integrated the λ att sites of P90C and RS6521, all as described (Simons et al., 1987). The recombinant phage (and plasmid parents) were: *rncO*⁺, λ RS473 (pRS1398); *rncO* Δ (1-R2), λ RS661 (pRS2594); *rncO* Δ (II), λ RS831 (pRS3086); *rncO* Δ (ss), λ RS822 (pRS3083); *rncO*(HP), λ RS826 (pRS3097); *rncO*(SHP), λ RS827 (pRS3098); *rncO39A/40U*, λ RS666 (pRS2667); *rncO121A/122U*, λ RS839 (pRS3102); *rncO39A/40U/121A/122U*, λ RS840 (pRS3103); *rncO* Δ (78-81), λ RS680 (pRS1859); *rncO* Δ (78-81ins), λ RS682 (pRS1864).

(Figs. 6, 7), and no RNase III cleavage of their RNAs was detected (not shown). Although we did not determine the secondary structures of these hybrid RNAs, a putative primer extension pause site near the 3' margins of both HP and SHP (not shown) suggested that the predicted hairpin structures were present, consistent with MFOLD analysis of these hybrid sequences (not shown).

These results show that a heterologous stem-loop structure can stabilize the *rnc* mRNA, but that the ex-

tent of stabilization is not predicted easily: HP has greater predicted thermodynamic stability than *rncO* stem-loop I, yet the latter confers greater metabolic stability. Moreover, in contrast to observations with the *ompA* leader (Emory et al., 1992), the *rncO* Δ (ss) mutation, which deletes the native 5' single-stranded *rnc* leader, has no effect on transcript stability, and there is little difference between the effects of HP and SHP (indeed, SHP is more stable than HP), making the role of single-stranded 5' leaders even less predictable.

Genetic analysis of structure II

Because structure II is rather large, the potential functions of its substructural elements were explored by examining the effects of several additional mutations. The *rncO* Δ (50-111) deletion, which removes both stem IIb and stem-loop IIc (leaving a 6-nt loop), did not appear to alter intrinsic *rnc* mRNA stability (Fig. 8A; cf. lanes 1 and 2 with 7 and 8), but reduced RNase III cleavage substantially (cf. lanes 9 and 10 with 15 and 16; we estimate that only \approx 50% of *rncO* Δ (50-111) transcripts are cleaved). Moreover, the *rncO* Δ (50-111) cleavage products included those with 5' termini corresponding to the upstream cleavage site (R1), as well as those corresponding to R2 (Fig. 8, lanes 15 and 16), unlike the *rncO*⁺ case, where only R2 termini are detected (lanes 9 and 10). Because these termini are detected by extension of a downstream primer, the *rncO* Δ (55-111) mutation must perturb cleavage at R2 in particular.

When 4 nt were deleted from structure IIc [*rncO* Δ (78-81)] or replaced by a synthetic 12-nt sequence [*rncO* Δ (78-81ins12)], there was no substantial effect on *rnc* mRNA stability (not shown) or *rnc*'-*lacZ* fusion expression (Fig. 7) in the presence or absence of RNase III. Like *rncO* Δ (II) (see above), the *rncO* Δ (45-122) mutation, which removes all but the bottom 7 bp of structure II, abolished RNase III cleavage (Fig. 8A, cf. lanes 5 and 6 with 13 and 14) without affecting intrinsic transcript stability (cf. lanes 1 and 2 and 5 and 6). Therefore, although no part of stem II governs intrinsic stability, stem IIa is required for RNase III control, stem IIb enhances RNase III cleavage efficiency, and stem-loop IIc has no obvious function.

The relative importance of sequence and structure at the RNase III cleavage site in stem IIa was also examined by mutation. The *rnc39A/40U* double point mutation, which disrupts the two GC bp that lie between the R1 and R2 cleavage sites (see Fig. 5), essentially abolished RNase III cleavage (Fig. 8B, cf. lanes 5 and 6) and control of *rnc*'-*lacZ* fusion expression (Fig. 7), as seen previously (Matsunaga et al., 1996). A similar double mutation on the opposite side of stem IIa (*rncO221A/222U*) has the same effect (Figs. 7, 8B). Importantly, the combination of these two double mutations, which is predicted to restore base pairing in

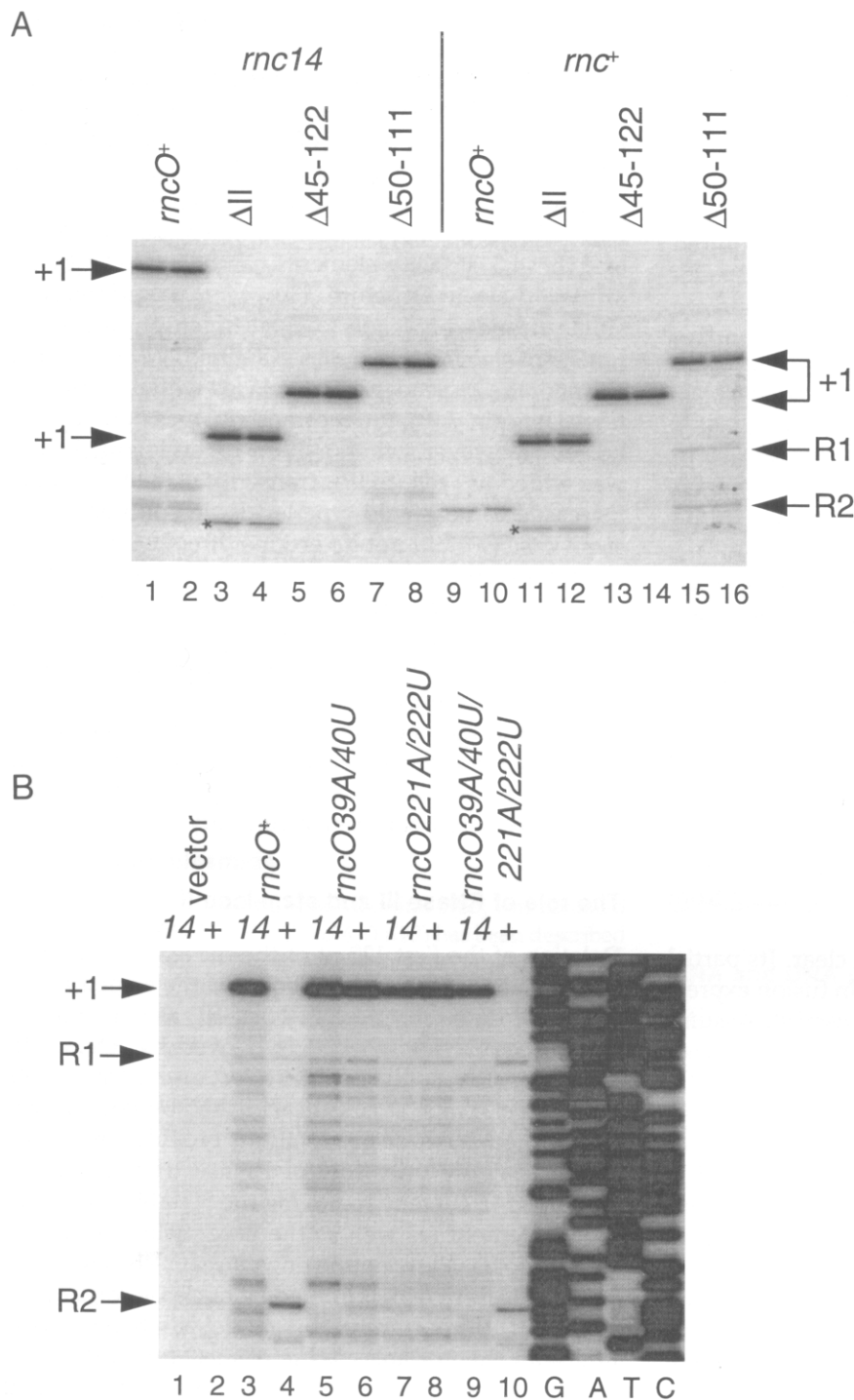


FIGURE 8. Effects of *rncO* mutations on RNase III cleavage. Total RNA extracted from RS6521 (*rnc14*) and P90C (*rnc+*) transformed with multicopy plasmids encoding the *rnc* gene and various *rncO* mutations was analyzed by primer extension (two independent samples in some cases) with the *rnc4* oligonucleotide as described (Matsunaga et al., 1996; see Figs. 1, 5, 6, and 7 for details of the mutations). Bands corresponding to the transcription start site (+1) and the upstream (R1) and downstream (R2) RNase III cleavage sites (Bardwell et al., 1989) are indicated. Asterisks mark the 3' margin of stem-loop I and probably result from reverse transcriptase pausing. **A:** Deletion mutations. Plasmids used were: *rncO+* (pRS1866), *rncOΔ(II)* (pRS3089), *rncOΔ(45-122)* (pRS3077), *rncOΔ(50-111)* (pRS3090). **B:** Point mutations. Plasmids used were: vector (pBR322), *rncO+* (*pACS1rnc105*), *rncO39A/40U* (pRS2733), *rncO121A/122U* (pRS3120), *rnc39A/40U/121A/122U* (pRS3121). The sequence ladder was generated with *rnc4* primer and pRS2249 template.

stem IIa without restoring primary sequence, almost completely restored RNase III cleavage and control (Figs. 7, 8B), showing the importance of base pairing at this site. It should be noted that these point mutations do not change bases that are part of the proposed consensus sequence for RNase III recognition (Krinke & Wulff, 1990; Nicholson, 1996).

Finally, Figure 5 shows that the *rnc* leader contains a short open reading frame (beginning with AUG at

+102) that overlaps the first two codons of the *rnc* gene (which begins with AUG at +161). To determine whether translation occurs at this ORF and affects expression or regulation of the *rnc* gene, we changed the AUG at +102 to ACG, which is a very weak initiation codon (Sussman et al., 1996). The ACG₁₀₂ mutation had no effect on *rnc'*-*lacZ* fusion expression or its regulation by RNase III (Fig. 7), and no effect was seen at the RNA level (not shown).

DISCUSSION

The *rncO* stability element

The *rncO* "operator" is a portable 5' RNA element that confers stability to the *rnc* mRNA as well as the heterologous *lac* and *kan* transcripts in the absence of RNase III, and contains all of the sequences required for RNase III control of these RNAs. Some of the details of *rncO* function have now been defined and are discussed most easily in the context of its secondary structure (Fig. 5). Neither the single-stranded 5' leader nor stem-loop II (which bears the RNase III cleavage site) is required for stabilization. However, removal of both stem-loops I and II (by mutations or RNase III cleavage) abolishes this function. Therefore, it follows that stem-loop I is required when stem-loop II is absent, although we did not determine if stem-loop I is required when stem-loop II remains intact. This raises an interesting question regarding the possible functional redundancy of stem-loops I and II. However, because both elements are removed by RNase III cleavage, such redundancy would not be relevant to RNase III control. In any case, stem-loop I (and/or II) is not sufficient for the *rncO* stabilizing function, because a downstream element, presumably stem-loop III, is also required. Therefore, structural elements in both the 5' and 3' regions of *rncO* are required, and the "minimal" *rncO* element can be defined as extending from nt +10 to +215.

The function of stem-loop III is not clear. Its partial deletion reduces both *rnc'*-*lacZ* protein fusion expression and the stability of the fusion transcript. Assuming that elongating ribosomes protect the *rnc* message from attack by RNases, stem-loop III may confer stability indirectly to the *rnc* transcript by promoting efficient translation initiation. Computer-assisted analysis of *rnc* RNA secondary structure (not shown) predicts that deletion of stem-loop III will sequester the *rnc* translation initiation region in dsRNA, which could reduce ribosome binding (de Smit & van Duin, 1994; Ma et al., 1994). Transcript stability in the corresponding *rnc'*-*kan* fusions was somewhat different, possibly reflecting subtle differences in RNA structure near the ribosome-binding site in these two contexts, although this was not apparent from computer analysis. Clearly, a more careful mutational analysis of stem-loop III will be required to determine its role in *rnc* mRNA translation and decay.

Although it is useful to define *rncO* function in terms of these particular structural elements, we point out that we have not yet analyzed the internal region of *rncO*, nor carefully addressed the relative importance of primary sequence versus secondary structure. Indeed, we have limited our analysis of *rncO* to its most basic structure and function, and a number of other issues remain to be resolved.

rncO is similar to the *ompA* stability element

Overall, our results with *rncO* are quite similar to those obtained by Belasco and colleagues working on the *E. coli ompA* gene (Emory et al., 1992; Hansen et al., 1994). The 5' untranslated leader of the *ompA* transcript contains two stem-loop structures, either of which confers stability to *ompA* as well as heterologous RNAs, and these 5' stability elements can be replaced by an artificial hairpin structure. However, the addition of single-stranded 5' leaders ≥ 5 nt in length decreased transcript stability in all cases examined. When the first 122 nt of the *rnc* leader were replaced with the same artificial hairpin (HP), the *rnc* transcript was partially stabilized. However, when a 10-nt heterologous leader was added as well (SHP), transcript stability actually increased to near wild-type levels, in contrast to the *ompA* case (we did not determine directly if these nucleotides were, in fact, unpaired). Moreover, deletion of 10 naturally unpaired nucleotides from the 5' end of the *rnc* transcript has no effect on stability. The differences between the *ompA* and *rnc* mRNA decay probably reflect differences in the decay pathways and their corresponding 5' structural requirements. In any case, we believe that the stabilizing or destabilizing effects of native or heterologous 5' structures or leaders cannot be predicted with much certainty.

The role of RNase III and stem-loop II

Deletion of the first 122 nt of the *rnc* leader produces a "pre-cleaved" RNA that decays at the same rate (in the presence or absence of RNase III) as does the native *rnc* transcript when it is cleaved by RNase III. Moreover, RNase III has little effect on *rnc* transcripts in which cleavage at *rncO* is abolished by point mutation. Together, these observations provide strong evidence that the only role of RNase III is to cleave stem-loop II, thereby removing the 5' stabilizing stem-loop I element (as well as the potentially redundant stem-loop II), allowing the downstream RNA to decay at its intrinsic rate (determined by nucleases other than RNase III). Importantly, this model is wholly consistent with the portable nature of *rncO* function.

We do note, however, that the "pre-cleaved" and RNase III-cleaved RNAs differ in a potentially important way: the "pre-cleaved" RNAs presumably bear 5' triphosphates, whereas RNase III-cleaved transcripts should bear a 5' monophosphate. This 5'-terminal difference apparently affects the decay of the ColE1 antisense RNA (Xu & Cohen, 1995), and may account for effects seen here, although we do not favor that interpretation.

It has been proposed that the RNase III cleavage generally occurs within a dsRNA structure at a moderately conserved consensus sequence positioned 10–14 bp from one end (Krinke & Wulff, 1990). The sequence

around the R1 and R2 sites in *rncO* matches this consensus sequence reasonably well, but these cleavage sites are only 6–7 bp from the end stem IIa. It is possible that stem IIb stacks onto IIa to extend the effective length of the helix. However, the *rncO* Δ (50–111) mutant RNA, which retains only the 15-bp stem IIa, is still cleaved by RNase III at the same sites (albeit with reduced efficiency), arguing against the “molecular ruler” model of Krinke and Wulff (1990). Similar conclusions were drawn from work on the bacteriophage T7 R1.1 substrate, where a reduction in the number of base pairs on either side of the RNase III cleavage site had no effect on the position of RNase III cleavage of T7 R1.1 in vitro (Chelladurai et al., 1993). The determinants of the RNase III recognition site remain to be defined.

MATERIALS AND METHODS

Materials

Restriction enzymes, RNA and DNA polymerases, and other modifying enzymes were purchased from New England Biolabs, Promega Biotech, or Stratagene. Antibiotics, media, and other chemicals were purchased from Sigma, Fisher, or Aldrich. Oligonucleotides were synthesized on a Beckman Oligo 1000 (some are mapped in Fig. 1).

Bacteria and plasmids

P90C [Δ (*lac-pro*) *thi ara*; Miller & Albertini, 1983] was obtained from J. Miller. RS6521 (P90C *rnc14::Tn10*) has been described (Matsunaga et al., 1996); the *rnc14* insertion mutation abolishes RNase III activity. pACS1 (obtained from D. Court) contains the 4.3-kb *'lep-rnc-era-recO-pdx]-acpS EcoR I* fragment from *E. coli* cloned into the *EcoR I* site of pBR322 (see Fig. 1). pACS1*rnc105* (also obtained from D. Court) is isogenic to pACS1 except for the *rnc105* point mutation, which abolishes RNase III activity (Bardwell et al., 1989; Matsunaga et al., 1996). pRS1398 and pRS1866 are derivatives of pACS1 and pACS1*rnc105*, respectively, that lack the *BamH I* fragments distal to the *rnc* gene (see Fig. 1).

The *rncO* Δ (1–R2) mutation was constructed by replacing *EcoR I-Hinc II* “*lep-rnc*” fragment from pRS1866 with a synthetic linker such that *rncP* and the first 122 nt of the *rnc* leader were replaced with the heterologous pOUT_{G8} promoter from IS10, which normally initiates transcription at two consecutive U residues (Simons et al., 1983; Case et al., 1988), but does not do so in this context (see the Results). The resulting plasmid (pRS2594) was found to contain an unexpected mutation in the –35 sequence of pOUT (GAGAAT instead of CAGAAT). The *rncO* Δ (II), *rncO* Δ (50–111), *rncO*(HP), and *rncO*(SHP) mutations were constructed by first generating PCR products with pRS1398 (*rnc*⁺) template appropriate mutant primers, and the products digested with *EcoR I* and *Hinc II* and used to replace the *EcoR I-Hinc II* fragment in pRS1866, yielding pRS3086, pRS3090, pRS3097, and pRS3098, respectively. The *rncO* Δ (*ss*) mutation was generated by M13 site-directed mutagenesis (Kunkel, 1985) with a mutant primer and M13mp18 template containing the *EcoR I-BamH I* “*lep-era*” fragment, and the mutant fragment

was then used to replace the corresponding segment of pRS1866, yielding pRS3083. The *rncO*ACG₁₀₂ and *rncO* Δ (45–122) mutations were introduced into pRS1866 by concurrent site-directed mutagenesis (“unique site elimination;” Deng & Nickoloff, 1992), using mutant primers to introduce the mutations and simultaneously eliminate the unique *Sca I* restriction site in the plasmid *bla* gene (without affecting ampicillin resistance), yielding pRS2816 and pRS3077, respectively. The *rncO* Δ (78–81) and the *rncO* Δ (78–81)*ins12* mutations were constructed by cutting the *Pst I* site at +77, trimming the resulting 3' overhanging ends with T4 DNA polymerase, and religating with T4 DNA ligase in the absence and presence of GGAAGATCTTC *Bgl II* linkers, ultimately yielding pRS1859 and pRS1864. The *rncO*121A/122U double mutant was constructed by PCR, to yield pRS3102. pRS3103 (*rncO*39A/40U/121A122U) was constructed by recombining appropriate fragments from pRS2667 and pRS3102. pRS2735, pRS3091, pRS3092, pRS3085, pRS3123, pRS3124, pRS2733, pRS3120, and pRS3121 are isogenic to pACS1*rnc105* and were constructed by replacing the *BstX I-Sal I* fragments from pRS2594, pRS3086, pRS3090, pRS3083, pRS3097, pRS3098, pRS2667, pRS3102, and pRS3103, respectively, with the *BstX I-Sal I* fragment from pACS1 (thereby restoring the *tet* gene in addition to *era*, *recO*, *pdxJ* and *acpS*; see Fig. 1). Construction of the *rncO*39A/40U double mutation in pRS2733 (isogenic to pACS1*rnc105*) has been described (Matsunaga et al., 1996); one of its parents, pRS2667, is isogenic to pRS1866. All *rncO* mutations and substitutions were confirmed by sequencing. Recombinant phage and some additional plasmid constructions are described in Figures 2, 3, and 7. Complete details of all strain constructions can be obtained upon request.

RNA and DNA methods

RNA extraction, primer extension analysis, and chemical half-life determinations were as described (Case et al., 1990; Matsunaga et al., 1996). To identify and quantitate 5' ends, primer extension analysis was used in preference to northern blots, because the decaying species have heterogeneous 3' termini, or RNase protection, where we generally obtain less precise 5' end identification. Dilution experiments with synthetic mRNAs and/or RNAs extracted from cells show that primer extension precision is within twofold between samples, and accurate over at least two orders of magnitude, as long as the same primer is used in any single comparison. All signals were quantitated with a Molecular Dynamics 445 SI PhosphorImager, where dilution experiments show linearity over more than three orders of magnitude. Sequence ladders were generated with a Sequenase Version 2.0 DNA Sequencing Kit (US Biochemicals). PCR and all other manipulations were done by standard methods (Sambrook et al., 1989). Oligonucleotides used for primer extension were *rncL* (5'-GGTTCGCTAACTGCTTCGCTGC-3'), *rncB* (5'-CCTGATGAT TAAAAGTGTAGCCC-3'), *rnc4* (5'-GTTTACTGCTGGCAC TAC-3'), *lacZ1* (5'-GGGATGTGCTGCAAGGC-3'), and *kan1* (5'-CCAAGCGCCGGAGAACC-3').

ACKNOWLEDGMENTS

We thank Don Court for his generous gift of several important strains, unpublished information, and much useful dis-

discussion; all members of our laboratory for helpful discussions and encouragement; and Philippe Régnier for critically reading the manuscript. J.M. was supported in part by an NIH Predoctoral Training Grant in Cellular and Molecular Biology (T32-GM1075) and an Ursula Mandel Award. This research was supported by grants from the National Institutes of Health (GM 50831) and the American Cancer Society (NP-863B).

REFERENCES

- Ahnn J, March PE, Takiff HE, Inouye M. 1986. A GTP-binding protein of *Escherichia coli* has homology to yeast RAS proteins. *Proc Natl Acad Sci USA* 83:8849-8853.
- Bardwell JCA, Regnier P, Chen SM, Nakamura Y, Grunberg-Manago M, Court DL. 1989. Autoregulation of RNase III operon by mRNA processing. *EMBO J* 8:3401-3407.
- Belasco J. 1993. mRNA degradation in prokaryotic cells: An overview. In: Belasco JG, Brawerman G, eds. *Control of messenger RNA stability*. San Diego: Academic Press. pp 3-12.
- Cannistraro VJ, Subbarao MN, Kennell D. 1986. Specific endonucleolytic cleavage sites for decay of *Escherichia coli* mRNA. *J Mol Biol* 192:257-274.
- Case CC, Roels SM, Gonzalez JE, Simons EL, Simons RW. 1988. Analysis of the promoters and transcripts involved in IS10 antisense RNA control. *Gene* 72:219-235.
- Case CC, Simons EL, Simons RW. 1990. The IS10 transposase mRNA is destabilized during antisense RNA control. *EMBO J* 9:1259-1266.
- Chelladurai B, Li H, Zhang K, Nicholson AW. 1993. Mutational analysis of a ribonuclease III processing signal. *Biochemistry* 32:7549-7558.
- Court D. 1993. RNA processing and degradation by RNase III. In: Belasco JG, Brawerman G, eds. *Control of messenger RNA stability*. San Diego: Academic Press. pp 71-116.
- Deng WP, Nickoloff JA. 1992. Site-directed mutagenesis of virtually any plasmid by eliminating a unique site. *Anal Biochem* 200:81-88.
- de Smit MH, van Duijn J. 1994. Control of translation by mRNA secondary structure in *Escherichia coli*. A quantitative analysis of the literature data. *J Mol Biol* 244:144-150.
- Ehresmann C, Baudin F, Mougél M, Romby P, Ebel JP, Ehresmann B. 1987. Probing the structure of RNAs in solution. *Nucleic Acids Res* 15:9109-9128.
- Ehretsmann CP, Carpousis AJ, Krisch HM. 1992. mRNA degradation in prokaryotes. *FASEB J* 6:3186-3192.
- Emory SA, Bouvet P, Belasco JG. 1992. A 5'-terminal stem-loop structure can stabilize mRNA in *Escherichia coli*. *Genes & Dev* 6:135-148.
- Gorski K, Roch JM, Krisch HM. 1985. The stability of bacteriophage T4 gene 32 mRNA: A 5' leader sequence that can stabilize mRNA transcripts. *Cell* 43:461-469.
- Hansen MJ, Chen LH, Fejzo MLS, Belasco JG. 1994. The *ompA* 5' untranslated region impedes a major pathway for mRNA degradation in *Escherichia coli*. *Mol Microbiol* 12:707-716.
- Inoue T, Cech TR. 1985. Secondary structure of the circular form of the *Tetrahymena* rRNA intervening sequence: A technique for RNA structure analysis using chemical probes and reverse transcriptase. *Proc Natl Acad Sci USA* 82:648-652.
- Kennell D, Reizman H. 1977. Transcription and translation initiation frequencies of the *Escherichia coli lac* operon. *J Mol Biol* 114:1-21.
- Kolodner R, Fishel RA, Howard M. 1985. Genetic recombination of bacterial plasmid DNA; effect of RecF pathway mutations on plasmid recombination in *Escherichia coli*. *J Bacteriol* 163:1060-1066.
- Krinke L, Wulff DL. 1990. The cleavage specificity of RNase III. *Nucleic Acids Res* 18:4809-4815.
- Kunkel TA. 1985. Rapid and efficient site-specific mutagenesis without phenotypic selection. *Proc Natl Acad Sci USA* 82:488-492.
- Ma CK, Kolesnikow T, Rayner JC, Simons EL, Yim H, Simons RW. 1994. Control of translation by mRNA secondary structure: The importance of the kinetics of structure formation. *Mol Microbiol* 14:1033-1047.
- March PE, Lerner CG, Ahnn J, Cui X, Inouye M. 1988. The *Escherichia coli* Ras-like protein (Era) has GTPase activity and is essential for cell growth. *Oncogene* 2:539-544.
- Matsunaga J, Dyer M, Simons EL, Simons RW. 1996. Expression and regulation of the *rnc* and *pxj* operons of *E. coli*. *Mol Microbiol*. Forthcoming.
- Mayford M, Weisblum B. 1989. Conformational alterations in the *ermC* transcript in vivo during induction. *EMBO J* 8:4307-4314.
- Miller JH, Albertini AM. 1983. Effects of surrounding sequence on the suppression of nonsense codons. *J Mol Biol* 164:59-71.
- Nicholson AW. 1996. Structure, reactivity, and biology of double-stranded RNA. *Prog Nucleic Acid Res Mol Biol* 52:1-65.
- Peterson C. 1991. Multiple determinants of functional mRNA stability: Sequence alterations at either end of the *lacZ* gene affect the rate of mRNA inactivation. *J Bacteriol* 173:2167-2172.
- Sambrook J, Fritsch EF, Maniatis T. 1989. *Molecular cloning: A laboratory manual*. Cold Spring Harbor, New York: Cold Spring Harbor Laboratory Press.
- Simons RW, Hoopes BC, McClure WR, Kleckner N. 1983. Three promoters near the termini of IS10: pIN, pOUT, and pIII. *Cell* 34:673-682.
- Simons RW, Houman F, Kleckner N. 1987. Improved single and multicopy *lac*-based cloning vectors for protein and operon fusions. *Gene* 53:85-96.
- Sussman JK, Masada-Pepe C, Simons EL, Simons RW. 1990. Vectors for constructing *kan* gene fusions: Direct selection of mutations affecting IS10 gene expression. *Gene* 90:135-140.
- Sussman JK, Simons EL, Simons RW. 1996. *Escherichia coli* translation initiation factor 3 discriminates the initiation codon in vivo. *Mol Microbiol* 21:347-360.
- Takiff HE, Chen SM, Court DL. 1989. Genetic analysis of the *rnc* operon of *Escherichia coli*. *J Bacteriol* 171:2581-2590.
- Xu F, Cohen SN. 1995. RNA degradation in *Escherichia coli* regulated by 3' adenylation and 5' phosphorylation. *Nature* 374:180-183.
- Zuker M. 1989. On finding all suboptimal foldings of an RNA molecule. *Science* 244:48-52.